Photodissociation of dimethyl sulfoxide at 193 nm in the gas phase

ARTICLE *in* THE JOURNAL OF PHYSICAL CHEMISTRY · DECEMBER 1993

Impact Factor: 2.78 · DOI: 10.1021/j100149a029

5 AUTHORS, INCLUDING:

Xirong Chen

15 PUBLICATIONS **188** CITATIONS

SEE PROFILE

Hongxin Wang

University of California, Davis

77 PUBLICATIONS **1,186** CITATIONS

SEE PROFILE

$SO(X\,^3\Sigma^-)$ production from the 193 nm laser photolysis of thionyl fluoride

Hongxin Wang, Xirong Chen and Brad R. Weiner [1]

Department of Chemistry, University of Puerto Rico, Box 23346, UPR Station, Rio Piedras, PR 00931, USA

Received 5 October 1993

The vibrational and rotational state distributions and the primary quantum yield of the $SO(X\,^3\Sigma^-)$ fragment following the laser photolysis of F_2SO at 193 nm have been measured by using laser-induced fluorescence spectroscopy on the $SO(B\,^3\Sigma^- - X\,^3\Sigma^-)$ transition. Molecular elimination of F_2 is the only energetically allowed channel to produce the SO fragment. The quantum yield measurement, $\Phi_{SO(X)}^{193\,nm} = 0.06 \pm 0.01$, suggests that other photochemical channels, e.g. FSO + F, must be operative as well.

1. Introduction

Sulfoxides and their halogenated analogs have played an important role in various areas of chemistry (see, for example, ref. [1]), and studies of their molecular structure and fundamental physical properties have been pursued during the past decades [2]. Thionyl fluoride (F_2SO) is the simplest of the stable three-coordinated sulfur compounds, and thus presents a compelling model for detailed dynamical studies. Photochemical investigations of thionyl chloride (Cl_2SO) have provided interesting dynamical results, i.e. the molecule exhibits multiple fragmentation pathways which vary with excitation wavelength [3–6], and provide an excellent model for concerted three-fragment dissociation. One of the goals of the experiments reported in this Letter is to examine whether similarities in the photochemistry of the isovalent species, F_2SO and Cl_2SO, are present.

Several studies have examined the spectroscopy and molecular structure of ground state F_2SO. Following the early work of Ferguson [7], microwave spectra of this molecule were reexamined by several research groups [8–10] to reveal its centrifugal distortion coefficients [8,9] and harmonic force field [10]. Vibrational frequencies were predicted by Lucas and Smith based on their harmonic force field results [10]. Both electron diffraction data and microwave spectroscopy establish that the geometry of the F_2SO molecule is consistent with C_s symmetry [2]. Microwave spectra in the vibrationally excited states have been obtained by Rimmer et al., revealing perturbation effects on the rotational constants [11]. High-resolution IR and Raman investigations of the vibrational spectroscopy of F_2SO including isotopic substitution effects, allowed O'Hara and Noftle to report high-accuracy frequencies for the six vibrational modes of thionyl fluoride [12]. In spite of the detailed structural investigations of this molecule, only a limited number of dynamical studies are reported in the literature [13,14].

The gas phase photochemistry of thionyl fluoride has not been previously reported, even though several studies on the photodissociation dynamics of thionyl chloride can be found in the literature [3–6]. By analogy to the 193 nm photodissociation of Cl_2SO, three photodissociation pathways might be assumed for F_2SO: (1) the simultaneous fission of two S–F bonds to give three fragments; (2) homolytic cleavage to produce FSO + F; and (3) the concerted molecular elimination of F_2. However, the simultaneous fission of both S–F bonds is not energetically allowed at 193 nm (148 kcal/mol). Thus, the molecular elimination channel [15],

$$F_2SO \rightarrow SO + F_2\,, \quad \Delta H_{rxn} = 119\ \text{kcal/mol}\,, \qquad (1)$$

[1] To whom correspondence should be addressed.

SSDI 00009-2614(93)E1277-N

is the only route which can directly produce nascent SO radicals following 193 nm irradiation. 193 nm photolysis of F_2SO may also lead to production of FSO, an important radical which has been the subject of limited experimental and theoretical studies [16,17]. The dearth of experimental work on this molecule results partially from the absence of a clean production methodology.

In this Letter, we report for the first time the observation of the production of $SO(X\,^3\Sigma^-)$ following the 193 nm irradiation of F_2SO under collision-free conditions. By measuring the internal state population distributions of the nascent photofragment(s), information about the detailed mechanism of the photodissociation of molecules can be revealed (see, for example, ref. [18]). Laser-induced fluorescence (LIF) spectroscopy has been effective in monitoring these internal state distributions [18]. We have employed the B–X transition here to measure the nascent vibrational, rotational and spin state distributions of the SO photofragment following photodissociation of F_2SO. Furthermore, the primary quantum yield of the SO-producing channel has been measured.

2. Experimental

The photodissociation experiments are performed on a standard two laser pump–probe apparatus, which has been described in detail previously [4,19]. Briefly, the gas phase sample, either neat or in buffer gas, is flowed through a glass four-way cross, which serves as the reaction chamber. Gas inlets are located on extension arms, which are used to reduce scattered light, while the vacuum outlet is located on the four-way cross. Only glass, polyethylene and stainless steel components are used for the reaction cell and inlet system to avoid heterogeneous decomposition of F_2SO. The reaction cell is evacuated by a mechanical pump and the pressure is monitored at the exit of the cell by a capacitance manometer. To maintain collision-free conditions, the pressure of the sample used in these experiments is between 0.030–0.040 Torr.

Photodissociation experiments have also been carried out in a stainless steel vacuum chamber fitted with a pulsed supersonic free jet. F_2SO, both pure and as a 10% mixture in helium, was introduced into the reaction chamber via a pulsed valve (General Valve; 0.5 mm diameter), which is mounted on the top of the chamber. The chamber is evacuated routinely to a background pressure of 1×10^{-7} Torr by a turbomolecular pump. We estimate the rotational temperature of the sample following the supersonic expansion to be ≈ 50 K for our experimental conditions.

Thionyl fluoride is photolyzed with the 193 nm output of an excimer laser (Lambda Physik LPX205i), operating on the ArF transition. Nascent SO radicals are monitored by LIF spectroscopy on the $B\,^3\Sigma^- - X\,^3\Sigma^-$ transition in the 237–295 nm region of the spectrum. The probe laser light in this region is generated by frequency doubling the output of a Lambda Physik FL3002 tunable dye laser with a β-BaB_2O_4 crystal, which is pumped by a Lambda Physik LPX205i excimer laser operated at 308 nm. The two lasers are collinearly counterpropagated along the extension arm axis to maximize the overlap region in the center of the reaction system. In the supersonic expansion experiments, the lasers cross the jet axis at a distance of 24 nozzle diameters from the valve. Laser-induced fluorescence is viewed at 90° relative to the laser beam axis by a photomultiplier tube through long-pass filters (Schott WG295, WG305). The output of the photomultiplier tube is processed and averaged by a gated integrator, digitized and sent to a personal computer for screen display, data storage and analysis. The delay time between the two lasers is controlled with a digital delay pulse generator and is fixed at a selected value while the frequency-doubled output of the dye laser was scanned to collect the total fluorescence signal, yielding a LIF excitation spectrum. The photolysis laser is operated at a repetition rate of 40 Hz and data are typically averaged for 10 laser shots.

Commercial thionyl fluoride (PCR, 99.5%, anhydrous grade) and helium (General Gases, 99.9%) are used without further purification.

3. Results

3.1. Vibrational state distribution

Under collision-free conditions ($P_{F_2SO}=0.040$

Torr; probe laser delay = 400 ns), the F_2SO is photolyzed by the output (10–50 mJ/cm^2) of a 193 nm excimer laser to produce SO($X\,^3\Sigma$). The LIF signal is found to have a linear dependence on the photolysis laser fluence, indicating that production of SO($X\,^3\Sigma$) was due to a single-photon process. No sulfur dioxide (SO_2), which gives a characteristic laser-induced fluorescence signal of its own in the probe laser wavelength region, is observed as an impurity in the F_2SO. The vibrational state population distribution (see fig. 1) of the nascent SO ($X\,^3\Sigma$, $v''=0$–5) fragment has been monitored by recording a LIF excitation spectrum of the SO($B\,^3\Sigma^-$–$X\,^3\Sigma^-$) transition in the region of 237–295 nm. Following the assignment of the (1, v'') bands, where $v''=0$–5, by using Colin's spectroscopic constants [20], the measured integrated band areas under this spectrum are normalized for the Franck–Condon factors [21] of the SO($B\,^3\Sigma^-$–$X\,^3\Sigma^-$) transition to obtain the relative vibrational state population of SO($X\,^3\Sigma^-$, $v''=0$–5). No nascent population is observed in the vibrational levels beyond $v''=5$, even though wavelengths corresponding to $v''=6$, 7 have been monitored (up to $v''=9$ is energetically allowed). In similar photodissociation studies of thionyl chloride, population in SO($X\,^3\Sigma^-$, $v''=6$, 7) has been measured by observation of the corresponding (1, v'') bands in the LIF excitation spectrum of SO(B–X) [6]. As shown in fig. 1, the vibrational state distribution is found to be inverted with a population maximum at $v''=2$, and without detectable population in $v''=0$, as measured from the (1, 0) band of the SO(B–X) transition. For the photodissociation of dimethyl sulfoxide (DMSO) at 193 nm, 14% of the nascent SO($X\,^3\Sigma$) is found in the vibrational ground state under similar photolysis conditions, which serves as an indicator of the LIF measurability of SO(X, $v''=0$) [22]. No signal is observed even when the (2, 0) and (3, 0) bands were probed, where larger Franck–Condon factors exist, again indicating no nascent population in the $v''=0$ vibrational state.

3.2. Rotational state distribution

The rovibronic transitions of SO($B\,^3\Sigma^-$–$X\,^3\Sigma^-$) have been used for the measurement of the nascent rotational state distributions of the SO($X\,^3\Sigma$) fragment. Figs. 2a and 2b are typical examples, comparing the nascent spectrum of SO($B\,^3\Sigma^-$, $v''=1$–$X\,^3\Sigma^-$, $v''=2$) transition band from the photodissociation of F_2SO following supersonic jet expansion and at room temperature. The former exhibits less rotational excitation of the SO photofragment. Only six branches, namely P_{11}, R_{11}, P_{22}, R_{22}, P_{33}, R_{33}, are strongly allowed in the SO($B\,^3\Sigma^-$–$X\,^3\Sigma^-$) electronic transition [23]. P_{22}, and/or R_{22} (e.g. fig. 3)

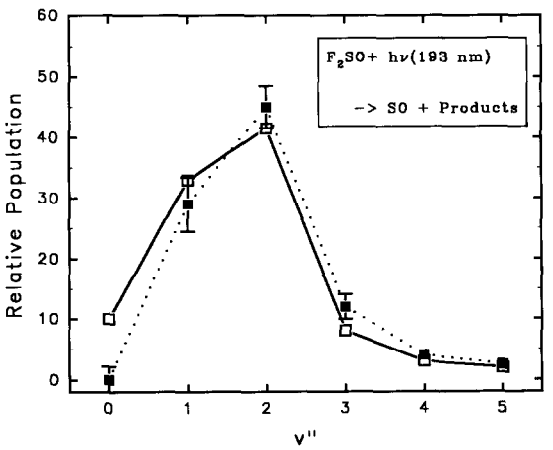

Fig. 1. Vibrational distribution of the nascent SO($X\,^3\Sigma^-$) fragment following the 193 nm photolysis of F_2SO. (■) represents the observed LIF distribution while (□) stands for a calculated distribution obtained by a Franck–Condon/Golden Rule best fit to the experimental data (see discussion).

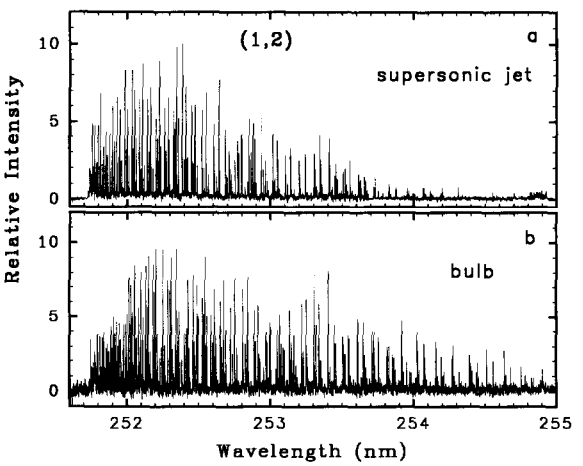

Fig. 2. LIF spectrum of the SO($B\,^3\Sigma^-$, $v'=1$–$X\,^3\Sigma^-$, $v''=2$) band resulting from the photolysis of F_2SO at 193 nm. (a) Following expansion in a supersonic jet, and (b) in the bulb, $P_{F_2SO}=0.040$ Torr.

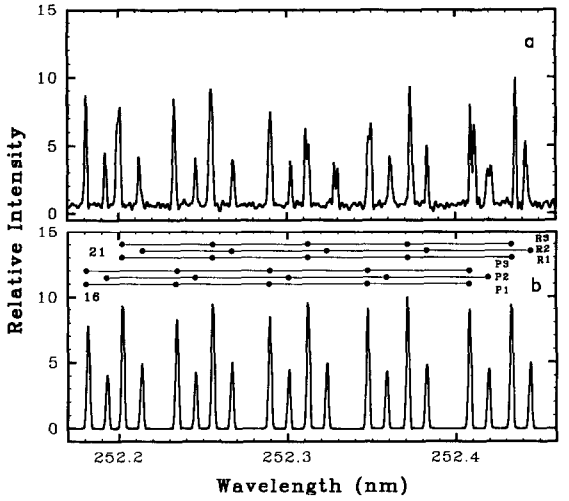

Fig. 3. (a) A portion of the laser-induced fluorescence spectrum of the (1, 2) band of the SO(B–X) transition following the 193 nm photolysis of 0.040 Torr F_2SO. A probe delay of 400 ns was used. (b) Spectral simulation of the same portion of the (1, 2) band of the SO(B–X) transition assuming a Boltzmann rotational state distribution (T_{rot} = 1400 K) and a Gaussian spectral line profile (fwhm = 0.25 cm^{-1}).

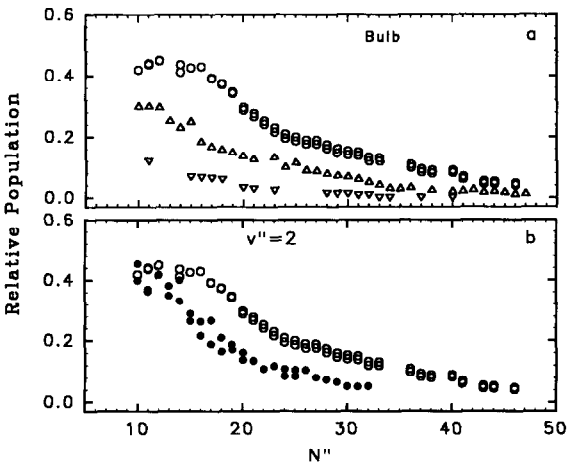

Fig. 4. (a) Comparison of the nascent rotational state distributions of the SO($X\,^3\Sigma^-$, $v''=1$–3) following the 193 nm laser photolysis of F_2SO in a bulb. (△) $v''=1$, 30%; (○) $v''=2$, 44%; (▽) $v''=3$, 12%. (b) Comparison of the nascent rotational state distributions of the SO($X\,^3\Sigma^-$, $v''=2$) state in (○) a bulb versus (●) a supersonic jet expansion.

are nearly resolved, for $v''=1$–3, and thus are used to directly measure the nascent relative rotational state populations in these vibrational bands. The assignment of the spectrum (cf. fig. 3) is based on a spectral simulation assuming a Boltzmann rotational state distribution and a Gaussian spectral line profile. The rovibronic transition frequencies are calculated by using Colin's spectroscopic constants [20]. The difference between the calculated line positions and our experimental measurements is less than 1 cm^{-1}. The population of a single rovibronic state, $P(v'', N'')$, can be obtained by normalizing the measured intensities to the Hönl–London factor for a $^3\Sigma^-$–$^3\Sigma^-$ transition and the rotational degeneracy $(2J''+1)$ [#1]. The rotational state distributions of the nascent SO($X\,^3\Sigma^-$, $v''=1$, 2, 3) are shown in fig. 4. The maximum of the rotational state distribution of the nascent SO($X\,^3\Sigma^-$) from the supersonically cooled F_2SO is found to shift towards lower N (cf. fig. 4b). These rotational state distributions can be approximately characterized with a standard Boltzmann function and the rotational temperatures, T_{rot}, for each vibrational level are shown in table 1. The rotational state distribution of SO($X\,^3\Sigma^-$, $v''=2$) has been obtained following the photolysis of supersonically cooled F_2SO, but not for the other vibrational levels because the signal-to-noise ratios are too small to give reliable results. The spin state distribution ratios, F_1/F_2, for the nascent SO($X\,^3\Sigma^-$) were observed to be close to unity for the vibrational states of $v''=1$–3, based on the agreement between a simulated laser-induced fluorescence spectrum, and the experimentally obtained spectrum, assuming equal spin state population distributions, $F_1=F_2=F_3$ (see fig. 3).

Table 1
The rotational state temperatures of the nascent SO($X\,^3\Sigma^-$; $v''=1$–3) following the 193 nm photodissociation of F_2SO

v''	Bulb	Supersonic jet
1	1200 ± 600 K	–
2	1400 ± 400 K	1000 ± 300 K
3	1300 ± 600 K	–

[#1] The Hönl–London factors were calculated by formulae given previously in ref. [24].

3.3. Primary quantum yield of $SO(X\,^3\Sigma^-)$

Quantum yield measurements of the $SO(X\,^3\Sigma^-)$ radicals provide an increased understanding of the photofragmentation of F_2SO. In our experiment, the $R_{22}(20)$ rovibronic line, 252.105 nm, in the $SO(B\,^3\Sigma^-,\ v'=1\text{–}X\,^3\Sigma^-,\ v''=2)$ transition is selected as the monitor wavelength. The (1, 2) vibronic transition is selected because it has the best signal-to-noise ratio in our spectra. The LIF signal intensities of $SO(X\,^3\Sigma^-)$ are recorded following photodissociation of F_2SO and SO_2, respectively under identical conditions (0.040 Torr sample gas and 2 μs delay). 1 Torr of helium is added as a buffer gas to ensure equilibration of the rotational and spin state distributions. The LIF signal intensity is the average of 2000 points and the data used for the quantum yield calculation is the average of 20 such signals. The averaged intensity for the nascent $SO(X\,^3\Sigma^-)$ is corrected by the absorption cross section (6.18×10^{-18} cm^2 for F_2SO [#2] and 8.12×10^{-18} cm^2 for SO_2 [25] at 193 nm) and the relative vibrational state population in the nascent $SO(X\,^3\Sigma^-,\ v''=2)$ for the two species [4]. The relative quantum yield for the nascent SO in its ground state, $X\,^3\Sigma^-$, produced in the 193 nm photodissociation of F_2SO is found to be $\Phi_{SO(X)}^{193\,nm}=0.06\pm0.01$, assuming unit efficiency in the production of nascent $SO(X\,^3\Sigma^-)$ from the photolysis of SO_2 [26]. The quantum yield measurement has also been checked at longer time delays (10–100 μs) and for other rotational lines, by monitoring the ratio of the LIF signals arising from SO_2 and F_2SO photolyses. The ratio does not change significantly in either case.

4. Discussion

The molecular elimination of F_2 is the only allowed photochemical route to the SO radical which can be produced in its ground electronic state, $X\,^3\Sigma^-$ and/or in its first excited state, $a\,^1\Delta$ ($\approx$18 kcal/mol above the ground state). The dissociation of F_2SO leading to SO+2F is energetically forbidden, so that both the concerted three-body fragmentation and a stepwise process resulting in SO+2F are ruled out as possible mechanisms for the production of the nascent SO fragment in the 193 nm photolysis of F_2SO. The quantum yield measurement indicates that 6% of the 193 nm photoactivated F_2SO directly produces SO in its ground state, $X\,^3\Sigma^-$. The absence of any growth in the quantum yield of $SO(X\,^3\Sigma^-)$ at longer time delays indicates that less than 1% of the photoactivated F_2SO produces $SO(a\,^1\Delta)$ directly. The small quantum yield for the nascent $SO(X\,^3\Sigma^-)$ is consistent with the difficulty of forming a strained three-center transition state prior to the molecular elimination. In the case of the photolysis of Cl_2SO at 248 nm, where an analogous energetic situation exists, $\leqslant$1% of the photoactivated Cl_2SO directly produces $SO(X\,^3\Sigma^-)$ via the molecular elimination channel [5,6]. Baum et al. also reported $\approx$3% of the SO photoproduct was directly produced in the $b\,^1\Sigma^+$ state following 248 nm photolysis of Cl_2SO [5]. $SO(b\,^1\Sigma^+)$ is not energetically accessible in these experiments. The primary quantum yield result obtained here for the 193 nm photolysis of F_2SO is consistent with the Cl_2SO observation following 248 nm irradiation. By analogy with the 248 nm photodissociation of Cl_2SO, the channel producing F+FSO may be responsible for the remaining 94% of the quantum yield, assuming all the photoactivated molecules dissociate [#3].

An energy balance analysis has been carried out, assuming a molecular elimination of F_2, since it is the only energetically allowed channel to produce SO. The energy disposal into the vibrational degree of freedom of the $SO(X\,^3\Sigma^-)$ photofragment can be evaluated as the sum of the energy partitioned into each vibrational level. We obtain $E_{vib}=6.6$ kcal/mol for the average vibrational energy of the nascent $SO(X\,^3\Sigma^-)$ following the 193 nm photodissociation of F_2SO. The average rotational energy in each vibrational level is taken as k_BT_{rot}, where k_B is the Boltzmann constant and T_{rot} is the rotational temperature from the nascent rotational state distribution. The total rotational energy is found to be 2 kcal/

[#2] The absorption cross section of F_2SO at 193 nm was obtained in our laboratory by using a Hewlett Packard (HP8452A) diode array spectrophotometer.

[#3] We have not observed any fluorescence at wavelengths > 300 nm coincident with the photolysis laser pulse. This does not conclusively rule out a non-negligible fluorescence quantum yield due to shorter wavelength emission.

mol by averaging over all the vibrational levels. The total internal state energy disposal into the SO radical is thus obtained to be 8.6 kcal/mol. The velocity of the nascent SO is estimated as 930 m/s by measuring its diffusion time out of the probe laser beam under low pressure conditions (e.g. 0.030 Torr). The translational energy of SO is thus approximated as 4.9 kcal/mol, and the total translational energy imparted to the photofragments is estimated as 11.2 kcal/mol, by assuming a geometry consistent with molecular elimination. This leaves 9.2 kcal/mol of the available energy unaccounted for, which is likely to be found in internal excitation of the nascent F_2 fragment. Vibrational excitation of F_2 may be expected, consistent with the large change of the F–F distance during the molecular elimination.

The inverted vibrational population distribution of the nascent $SO(X\,^3\Sigma^-)$ indicates that the dissociation of F_2SO occurs on a timescale that is competitive with intramolecular vibrational relaxation. Since the photofragmentation occurs via a molecular elimination of F_2, a three-center transition state seems likely. Modelling the nascent SO vibrational distribution is useful in addressing the geometry of the parent molecule prior to the dissociation [4,6,27]. An inverted vibrational distribution from a chemical reaction can be approached by a Franck–Condon/Golden Rule model, which has been described previously [4,6,27]. Application of this simple model to the photodissociation of SO_2 has been shown to give credible results [4]. Unlike in the case of SO_2, we find that the SO bond length in the ground state of F_2SO can rationalize our experimental results of an inverted vibrational distribution (cf. fig. 1). By using a bond length of 1.42 Å and a trial vibrational frequency of 1450 cm^{-1}, the Franck–Condon/Golden Rule model produces a calculated vibrational distribution which is in close agreement with our measurement, as shown in fig. 1. These parameters are in close agreement with the reported values for the ground state F_2SO ($d_{SO}=1.42$ Å and $\nu=1329$ cm^{-1}) [12]. Since a direct dissociation is not consistent with the three-center transition state necessary for the molecular elimination, we conclude that the 193 nm Franck–Condon excitation of F_2SO does not lengthen the SO bond, significantly.

The peak of the nascent rotational state distribution of $SO(X, v''=2)$ following the photolysis of supersonically expanded F_2SO is found to shift to lower N (by about 10 rotational levels), in comparison with the room temperature photolysis of F_2SO. The higher photofragment rotational excitation in the latter case can be ascribed to the contribution from the initial rotational angular momentum of the parent molecule. This result provides evidence for a strong coupling between the initially excited state and the dissociative state. This case is still unusual, as the effect of parent angular momentum on the photofragment rotational state distribution(s) is often washed out in predissociative cases [28].

5. Summary and conclusions

The state distributions and quantum yield of the nascent $SO(X\,^3\Sigma^-, v'')$ have been measured by using laser-induced fluorescence spectroscopy following the photodissociation of F_2SO at 193 nm. The vibrational distribution of the nascent SO(X) fragment has been found to be inverted with a population maximum at $v''=2$, indicating a rapid dissociation process. The molecular elimination of F_2 from F_2SO is the only energetically allowed channel in this case, which is consistent with the observed energy partitioning, and suggests that the nascent F_2 fragment is born with significant vibrational excitation. A Franck–Condon model best fits the observed vibrational state distribution when the SO bond length is similar to that of the ground state F_2SO. The primary quantum yield, $\Phi_{SO(X)}^{193\,nm}=0.06\pm0.01$, has been measured, suggesting that the non-SO-producing channel $F_2SO \rightarrow FSO+F$ is most likely the major photochemical channel.

Acknowledgement

The experiments performed here were done in conjunction with Puerto Rico Laser and Spectroscopy Facility at the University of Puerto Rico, under the auspices of NSF-EPSCoR Program. Acknowledgements are also made to the Air Force Office of Scientific Research which has generously supported this research through Grants F49620-92-J-0406 and F49620-93-1-0110. The authors would also like to thank Manuel A. Rivera who assisted our work by

taking the absorption spectrum of F_2SO.

References

[1] S. Patai, Z. Rappoport and C. Stirling, eds., The chemistry of sulphones and sulphoxides (Wiley, New York, 1988).
[2] I. Hargittai, The structure of volatile sulphur compounds (Reidel, Dordrecht, 1992).
[3] M. Kawasaki, K. Kasatani, H. Sato, H. Shinohara, N. Nishi, H. Ohtoshi and I. Tanaka, Chem. Phys. 91 (1984) 285.
[4] X. Chen, F. Asmar, H. Wang and B.R. Weiner, J. Phys. Chem. 95 (1991) 6415.
[5] G. Baum, C.S. Effenhauser, P. Felder and J.R. Huber, J. Phys. Chem. 96 (1992) 756.
[6] H. Wang, X. Chen and B.R. Weiner, J. Phys. Chem. 97 (1993), in press.
[7] R.C. Ferguson, J. Am. Chem. Soc. 76 (1954) 850.
[8] I. Yamaguchi, O. Ohashi, H. Takahasi, T. Sakaizumi and M. Onda, Bull. Chem. Soc. Japan 46 (1973) 1560.
[9] A. Dubrulle and J.L. Destombes, J. Mol. Struct. 14 (1972) 461.
[10] N.J.D. Lucas and J.G. Smith, J. Mol. Spectry. 43 (1972) 327.
[11] D.F. Rimmer, J.G. Smith and D.H. Whiffen, J. Mol. Spectry. 45 (1973) 114.
[12] T.J. O'Hara and R.E. Noftle, J. Fluorine Chem. 20 (1982) 149.
[13] J.R. Morton and K.F. Preston, J. Chem. Phys. 58 (1973) 2657.
[14] K. Garber and B. Ault, Inorg. Chem. 22 (1983) 2509.
[15] G.A. Takacs, J. Phys. Chem. Ref. Data 16 (1987) 1.
[16] S. Sakai and K. Morokuma, Chem. Phys. 52 (1980) 33.
[17] Y. Endo, S. Saito and E. Hirota, J. Chem. Phys. 74 (1981) 1568.
[18] R. Bersohn, in: Molecular photodissociation dynamics, eds. M.N.R. Ashfold and J.E. Baggott (Royal Society of Chemistry, London, 1987) pp. 1–30.
[19] K.I. Barnhard, A. Santiago, M. He, F. Asmar and B.R. Weiner, Chem. Phys. Letters 178 (1991) 150.
[20] R. Colin, Can. J. Phys. 47 (1969) 979; J. Chem. Soc. Faraday Trans. II 78 (1982) 1139.
[21] W.H. Smith and H.S. Liszt, J. Quant. Spectry. Radiative Transfer 11 (1971) 45.
[22] X. Chen, H. Wang, B.R. Weiner, M. Hawley and H.H. Nelson, J. Phys. Chem. 97 (1993), in press.
[23] G. Herzberg, Molecular spectra and molecular structure, Vol. 1. Spectra of Diatomic Molecules (Krieger, New York, 1989).
[24] J.B. Tatum, Can. J. Phys. 44 (1966) 2944.
[25] H. Okabe, Photochemistry of small molecules (Wiley, New York, 1978).
[26] H. Kanamori, E. Tiemann and E. Hirota, J. Chem. Phys. 89 (1988) 621.
[27] M.J. Berry, Chem. Phys. Letters 29 (1974) 323, 329.
[28] R. Schinke, Comments At. Mol. Phys. 23 (1989) 15.